

## RESEARCH ARTICLE

### Biomechanics of spontaneous overground walk-to-run transition

Veerle Segers<sup>1,\*</sup>, Kristof De Smet<sup>1</sup>, Ine Van Caekenbergh<sup>1,2</sup>, Peter Aerts<sup>1,2</sup> and Dirk De Clercq<sup>1</sup>

<sup>1</sup>Department of Movement and Sport Sciences, Ghent University, Watersportlaan 2, B-9000 Gent, Belgium and

<sup>2</sup>Department of Biology – Functional Morphology, University of Antwerp (CDE), Universiteitsplein 1, B-2610 Wilrijk, Belgium

\*Author for correspondence (veerle.segers@ugent.be)

#### SUMMARY

The purpose of the present study was to describe the biomechanics of spontaneous walk-to-run transitions (WRTs) in humans. After minimal instructions, 17 physically active subjects performed WRTs on an instrumented runway, enabling measurement of speed, acceleration, spatiotemporal variables, ground reaction forces and 3D kinematics. The present study describes (1) the mechanical energy fluctuations of the body centre-of-mass (BCOM) as a reflection of the whole-body dynamics and (2) the joint kinematics and kinetics. Consistent with previous research, the spatiotemporal variables showed a sudden switch from walking to running in one transition step. During this step there was a sudden increase in forward speed, the so-called speed jump ( $0.42\text{ m s}^{-1}$ ). At total body level, this was reflected in a sudden increase in energy of the BCOM ( $0.83\pm 0.14\text{ J kg}^{-1}$ ) and an abrupt change from an out-of-phase to an in-phase organization of the kinetic and potential energy fluctuations. During the transition step a larger net propulsive impulse compared with the preceding and following steps was observed due to a decrease in the braking impulse. This suggests that the altered landing configuration (prepared during the last 40% of the preceding swing) places the body in an optimal configuration to minimize this braking impulse. We hypothesize this configuration also evokes a reflex allowing a more powerful push off, which generates enough power to complete the transition and launch the first flight phase. This powerful push-off was also reflected in the vertical ground reaction force, which suddenly changed to a running pattern.

Supplementary material available online at <http://jeb.biologists.org/cgi/content/full/216/16/3047/DC1>

Key words: gait transition, human, kinetics, kinematics.

Received 19 February 2013; Accepted 11 April 2013

#### INTRODUCTION

Cyclic terrestrial locomotion in animals is often characterized by the presence of different gaits, each of which is used for a specific range of velocity. This implies that transitions from one gait to another must occur when animals speed up or slow down. Humans walk at a slow speed, but switch spontaneously to running when moving faster. Thus far, many experimental studies on the mechanics of this transition have been carried out, either using a steady protocol (steady locomotion on a treadmill with a stepwise velocity increase) (e.g. Hreljac, 1993; Raynor et al., 2002; Ivanenko et al., 2006; Hreljac et al., 2007; Prilutsky and Gregor, 2001; Ganley et al., 2011) or by imposing a constant (relatively small) acceleration on a treadmill (e.g. Thorstensson and Rotherthson, 1987; Diedrich and Warren, 1995; Turvey et al., 1999; Segers et al., 2006; Segers et al., 2007a; Hreljac et al., 2007; Nimbarte and Li, 2011) or overground (e.g. Hreljac et al., 2008; Segers et al., 2007b).

Recently, De Smet and colleagues (De Smet et al., 2009a; De Smet et al., 2009b) introduced a novel approach to study the walk-to-run transition (WRT). In their studies, subjects were instructed to start walking and to accelerate within the walking pace. Remarkable differences from previous findings with the more controlled setups emerged: during the voluntary approach to transition, spontaneously chosen accelerations were higher ( $0.7\text{ m s}^{-2}$ ) than those previously imposed [up to  $0.18\text{ m s}^{-2}$ ; except for two recent treadmill studies (Van Caekenbergh et al., 2010a; Van Caekenbergh et al., 2010b) with imposed accelerations up to

$0.5\text{ m s}^{-2}$ ]; the transition speed of  $2.7\text{ m s}^{-1}$  ( $\pm 0.2\text{ m s}^{-1}$ ) is considerably higher than that registered in stepwise steady-state or constantly accelerating protocols (ranging from  $1.9$  to  $2.3\text{ m s}^{-1}$ ) (Li, 2000; Li and Hamill, 2002). This on average 30% increase in transition speed is predominantly caused by the presence of a large speed jump of  $0.4\text{ m s}^{-1}$  during the transition step (De Smet et al., 2009b).

Moreover, despite the absence of any imposed boundary condition, low intraindividual and interindividual variability indicates that test subjects execute the spontaneous transition in a similar way: first, there is a rapid, primarily frequency modulated acceleration towards the preferred walking speed; then, the increase in velocity is more and more due to an increase in step length; and finally, just before transition, acceleration is entirely step length modulated (i.e. saturation of the cycle frequency). This consistent behaviour observed during the spontaneous overground transition experiments probably reflects an intrinsic control or self-organization for the human walk-to-run transition. Such insight into the interplay between neuromuscular control and intrinsic system mechanics (i.e. neuromechanics) (cf. Nishikawa et al., 2007) of the (human) locomotor apparatus may further be useful for fundamental (motor control) and applied (rehabilitation, robotics) research.

To date, these intrinsic biomechanistic aspects of transitions are still largely unknown. This study presents a biomechanical analysis, up to the joint and muscular level, of the spontaneous overground transition from walking to running. Segmental kinematics, whole-body dynamics (ground reaction forces, mechanical energy

fluctuations), joint dynamics (joint moments and powers) and muscle activation patterns were combined and interpreted to uncover and to better understand the key events that lead to the subconscious, voluntary gait transition in humans.

## MATERIALS AND METHODS

### Subjects

Seventeen female subjects (height  $169.7 \pm 8.5$  cm, mass  $61.3 \pm 6.0$  kg) participated in the present study after having given informed consent. The ethical committee of the Ghent University Hospital approved the experimental protocol.

### Procedure

Subjects performed WRT trials on a 30 m long walkway. They were asked to start from standing, and then to progress with a spontaneously chosen acceleration to a walking, a transitional and finally a running mode. This way, subjects adapted their progression speed freely (De Smet et al., 2009b) and broke spontaneously into a run at an unpredicted or non-prescribed speed.

This protocol is practically impossible on a treadmill, unless a treadmill on demand is used, which automatically adapts its speed to the subject's actions. Moreover, Van Caekenberghe and colleagues (Van Caekenberghe et al., 2013) showed that accelerating overground and on treadmill are largely different because of the altered mechanics. Before the test, all subjects were familiarized with the protocol.

### Data collection

Kinematic data were collected at 200 Hz using 12 infrared cameras (Qualisys Pro Reflex, Gothenburg, Sweden) and Qualisys software (anatomical and tracking) markers were placed on the subject. Anatomical markers were placed on the medial and lateral malleolus, the first and the fifth metatarsal, the medial and lateral part of the calcaneus, the medial and lateral femoral condyles, the greater trochanter, the anterior superior iliac spine, the top of the acromion, the medial and lateral epicondyle of the humerus and the wrist. Tracking markers were placed on the shank (four), the thigh (four), the coccyx, the seventh cervical vertebra, the upper arm (two) and the lower arm (two).

Within the recording volume, ground reaction forces (GRFs) were measured using six force plates (one  $2 \times 0.4$  m AMTI, one  $0.6 \times 0.4$  m Kistler, two  $1.0 \times 0.4$  m AMTI and two  $0.5 \times 0.5$  m AMTI). These were built in the walkway, in such a manner that they were invisible to the subjects to avoid targeting for the force plates.

Across successive trials, the starting position with respect to the recording volume was adjusted such that kinematics could be recorded for seven subsequent steps, with the transition occurring in the middle of this sequence. Steps are defined as the events between two successive touchdowns of the contralateral feet. Steps prior to transition are indicated with negative signs (step -3, step -2, step -1). Steps after transition are indicated with positive signs (step +1, step +2). The transition step (step 0) was defined as the first step with a flight phase, which proved to coincide with the switch from a pendular to a bouncing gait (see Segers et al., 2007b). Trials were repeated until five successful WRTs (according to the above conditions) were registered per subject.

Speed was recorded over the entire 30 m walkway using a Noptel Distance laser (CMP2-30, Oulu, Finland) at 1000 Hz. This laser measures distance based on time delays of reflected pulsed infrared light. The raw position signal was filtered using a Butterworth low-pass filter (10 Hz cut-off frequency) and speed was calculated as the first derivative of distance with respect to time. The distance

laser was placed at lumbar height of the subject, directing the laser beam level with the ground.

### Data analysis

A seven-segment model (feet, shanks, thighs, trunk) was developed to calculate kinematics and kinetics using Visual 3D (Germantown, MD, USA), a biomechanical analysis and modelling software using motion capture data. Ankle, knee and hip joint kinematics and kinetics (net joint moments and powers) were calculated. The trunk angle was computed with respect to the laboratory coordinate system (anteversion/retroversion). The total body centre-of-mass (BCOM) was derived from the seven segments using standard Visual 3D segment parameters.

Step data were averaged over different trials per subject as intra-individual variability was low for the kinematic as well as for the spatiotemporal variables. Kinematic variables were analysed within steps. Step +2 mostly was not executed inside the recording zone. However, for the steps that were recorded, only small differences in spatiotemporal and kinematic aspects were found between step +1 and step +2, and therefore inverse dynamics were done for the last two walking steps, the transition step and the first running step (step -2 to step +1).

Forces and force impulses were normalized to body weight to obtain dimensionless quantities. In order to compare the results to the literature, energetic, joint moments and powers were normalized to body mass.

All data were analysed using the SPSS 16.0 package. A repeated measures ANOVA was used to check for differences ( $P \leq 0.05$ ) between steps.

### Post hoc electromyogram measurements

Five subjects performed three spontaneous overground WRTs *post hoc*. Spatiotemporal and GRF data were comparable to those of the original study. Subjects were equipped with zero Wire electromyogram (EMG) electrodes (Aurion, Milan, Italy). Electrodes were attached at the m. vastus medialis according to the guidelines of the International Society of Electrophysiology and Kinesiology (ISEK). EMG measurements were rectified and band-pass filtered (2–300 Hz), a linear envelop of EMG was calculated and then normalized to the maximal value obtained during the transition trial.

## RESULTS

### Spatiotemporal characteristics

Subjects took on average  $4.9 \pm 1.0$  walking steps before making the WRT. The mean time to transition was  $2.25 \pm 0.41$  s. The transition speed was  $2.74 \pm 0.25$   $\text{m s}^{-1}$ . Speed further increased during step +1 ( $2.98 \pm 0.34$   $\text{m s}^{-1}$ ) and step +2 ( $3.12 \pm 0.40$   $\text{m s}^{-1}$ ), after which a steady-state running speed ( $3.18 \pm 0.04$   $\text{m s}^{-1}$ ) was reached. The highest step-to-step speed increase ( $0.42$   $\text{m s}^{-1}$ ) was observed during the transition step (step 0), which was also characterized by an increased step length and a decreased step frequency. In the approach to the transition step, step frequency and step length increased gradually, and after the transition the step frequency remained constant at 2.6 Hz and the rather small speed increase was accomplished by an increase in step length. The spatiotemporal data are consistent with previous findings during a spontaneous overground WRT (De Smet et al., 2009a; De Smet et al., 2009b). More data are available in supplementary material Table S1.

### Mechanical energy fluctuations of the BCOM

Total mechanical energy (Fig. 1) increased  $0.47 \pm 0.07$   $\text{J kg}^{-1}$  during step -2,  $0.34 \pm 0.06$   $\text{J kg}^{-1}$  during step -1,  $0.83 \pm 0.14$   $\text{J kg}^{-1}$  during step

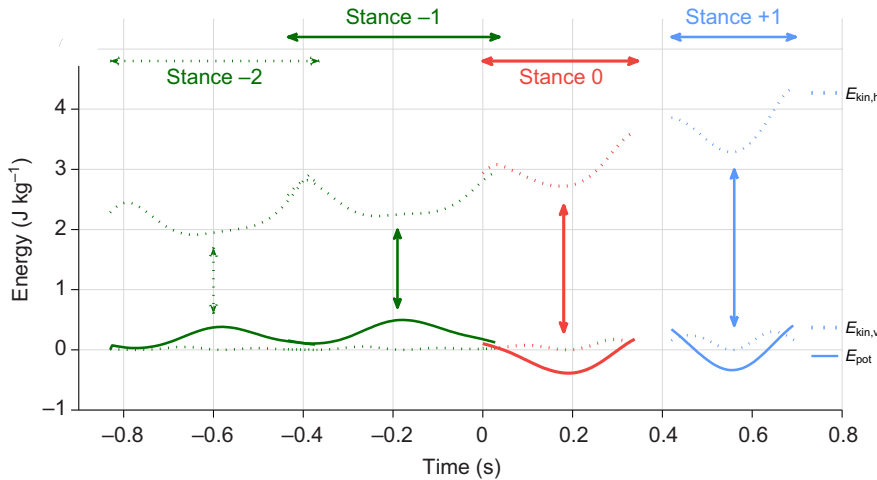


Fig. 1. Energy fluctuations of the body centre-of-mass (BCOM) during the spontaneous walk-to-run transition (WRT). Solid lines represent the potential energy ( $E_{pot}$ ), indicating the switch from an inverted pendulum (step -2 and step -1) to a spring-mass (step 0, step +1). Upper dotted lines represent the horizontal kinetic energy ( $E_{kin,h}$ ); lower dotted lines represent the vertical kinetic energy ( $E_{kin,v}$ , maximum  $0.33 \text{ J kg}^{-1}$ ). The arrows indicate the out-of-phase energy fluctuations of BCOM for step -2 and step -1 (green) and the in-phase energy organization of gravitational  $E_{pot}$  and  $E_{kin}$  for step 0 and step +1 (red and blue). Time 0 is the heel contact transition step.

0 and  $0.59 \pm 0.12 \text{ J kg}^{-1}$  during step +1. Most of this total energy was invested in the increase in horizontal kinetic energy: 86.16% in step -2, 108.35% in step -1 (>100%, because the increase in horizontal kinetic energy even exceeds the total energy increase because of a decrease in gravitational potential energy), 83.74% for step 0 and 86.00% for step +1.

### GRFs

The time series of both the horizontal and the vertical GRF of the transition step have more in common with the GRF for running than for walking (Fig. 2; a time-normalized version of this figure is presented in supplementary material Fig. S1).

The absolute value of the braking horizontal force of step 0 was smaller than that in the accelerated walking and running steps. The absolute value of the normalized braking impulse changed little from step -2 to step -1 ( $0.27 \pm 0.04$  versus  $0.26 \pm 0.06 \text{ N s kg}^{-1}$ ), but decreased significantly for the transition step ( $0.18 \pm 0.05 \text{ N s kg}^{-1}$ ). At step +1, braking impulses (in absolute terms) were significantly higher again ( $0.24 \pm 0.03 \text{ N s kg}^{-1}$ ) compared with those at the transition step. The impulse of the propulsive force did not differ significantly between steps, resulting in a net forward accelerating impulse of  $0.12 \pm 0.03 \text{ N s kg}^{-1}$  for step -2,  $0.14 \pm 0.07 \text{ N s kg}^{-1}$  for step -1,  $0.23 \pm 0.10 \text{ N s kg}^{-1}$  for step 0 and  $0.18 \pm 0.06 \text{ N s kg}^{-1}$  for step +1. This implies a significantly higher net propulsive impulse for step 0 compared with all other steps and a significantly higher net propulsive impulse for step +1 compared with the walking steps.

The time integral of the vertical GRF minus body weight, when the vertical GRF exceeds body weight (filled area in Fig. 2B), is the summation of two components in walking (double hump), whereas this is only one area in the transition step and the subsequent running step. In order to compare these impulses, the vertical impulse of step 0 and step +1 was divided into a vertical impulse during the braking phase and a vertical impulse during the propulsive phase. The results are shown in Fig. 3.

For step -2 this equals  $2.16 \pm 0.72 \text{ N s kg}^{-1}$  (braking phase  $1.3 \text{ N s kg}^{-1}$  + propulsive phase  $0.86 \text{ N s kg}^{-1}$ ), for step -1 this was  $2.25 \pm 0.74 \text{ N s kg}^{-1}$  ( $1.63 + 0.62 \text{ N s kg}^{-1}$ ),  $3.01 \pm 0.61 \text{ N s kg}^{-1}$  for step 0 ( $1.12 + 1.87 \text{ N s kg}^{-1}$ ) and  $3.54 \pm 0.51 \text{ N s kg}^{-1}$  for step +1 ( $1.80 + 1.87 \text{ N s kg}^{-1}$ ).

### Kinematics

The stick figures in Fig. 4 are based upon the mean kinematics of all test subjects.

The ankle of the stance limb showed larger maximal dorsiflexion velocity followed by a faster plantar flexion after mid-stance (Fig. 5A; a time-normalized version of this figure is presented in supplementary material Fig. S2) during step 0 and step +1 compared with step -2 and step -1. For the knee, a larger maximal flexion velocity followed by a high knee extension velocity (Fig. 5B) was found during stance of step 0 and step +1, compared with steps -2 and -1. Anteversion of the trunk was larger ( $\pm 7$  deg) during step -1 (compared with step -2) and reached its maximum ( $\pm 20$  deg) at 50% of the contact phase of step 0.

Kinematic adaptations can be observed during the swing preceding heel strike of the transition step. During the last 40% of swing (the period from toe-off of step -2 towards heel contact of

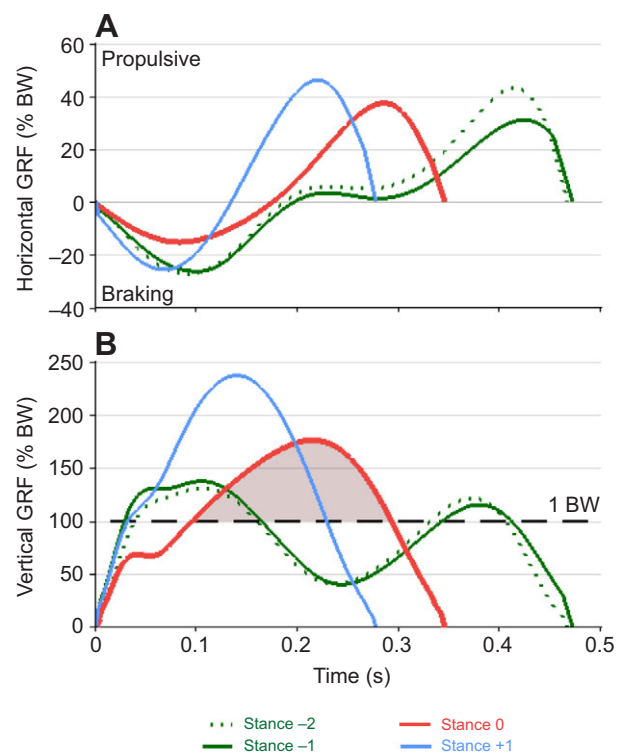


Fig. 2. Ground reaction forces (GRFs) during the spontaneous WRT. (A) Horizontal (fore-aft) GRFs. (B) Vertical GRFs. The shaded area represents the time integral of the vertical GRF minus body weight (BW), when the vertical GRF exceeds body weight.

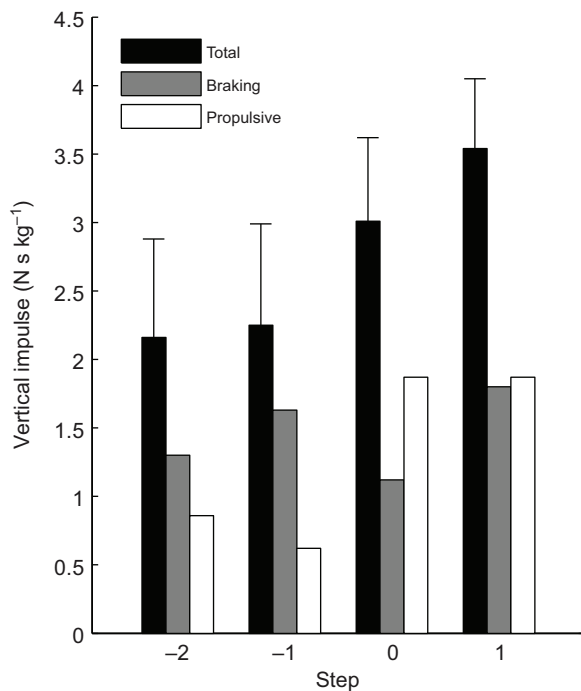


Fig. 3. Vertical impulses during the spontaneous WRT. Bars indicate the mean (+1 s.d.) vertical impulse during the entire step (total), and during the braking phase and propulsive phase.

step 0) there was an increase in flexion of the knee and hip of the swinging limb, leading to an altered landing configuration at heel contact of step 0: the stance limb knee and hip were more flexed and the trunk leant further forward compared with that during heel contact of step -1 (Fig. 4B).

#### Joint kinetics

The time series of joint moment (Fig. 6) and power profiles (Fig. 7) during the stance phases of the walking (step -2 and -1) and running steps (step +1) were compared with data from the literature and largely resemble the known profiles for these gaits (e.g. Winter, 1983; Winter, 1991; Farley and Ferris, 1998; Lee and Hidler, 2008). Time-normalized versions of these figures are presented in supplementary material Figs S3 and S4, respectively. We further focus on the transition step below.

In general, the evolution of joint moments (Fig. 6) during stance phase of the transition step shows time profiles (red curves) that differ from those of walking but strongly resemble those of running (blue curve), especially when the effect of the 0.08 s longer stance

duration in step 0 is taken into account (i.e. time-normalized profile differences are even smaller). Comparing the transition step and the subsequent running step, the peak value of the knee extension joint moment does not differ, whereas a smaller peak extension moment in the ankle and a smaller peak hip flexion moment are found.

Looking at the joint power curves (Fig. 7), step 0 again differs from the preceding walking steps and resembles running step +1: after a distinct negative power peak, positive extension power is generated in the ankle and the knee during push off occurring in the second half of the transition step. Although the ankle and knee peak extension power appear to be higher in step 0, the positive work delivered during steps 0 and +1 (time integrals of A1 and K3 phases, Table 1) in the ankle and the knee is comparable. For the hip, smaller joint power amplitudes are found but the overall shape of the time series is comparable. For the ankle, after the small initial plantar flexion velocity at heel contact and a distinct dorsiflexion velocity (Fig. 5C), a positive plantarflexion velocity in combination with a dominant extension moment during push-off results in power generation during the second half of stance (Fig. 7C, A1 phase). The work delivered during A1 is significantly larger for step 0 and step +1 compared with the previous walking steps (see Table 1). The flexion–extension movement of the knee is accompanied by an extension moment, giving rise to power absorption (Fig. 7B, K2 phase) before mid-stance and power generation afterwards (Fig. 7B, K3 phase). The power absorption and the positive work in the knee during push-off are significantly larger for step 0 and step +1 compared with the walking steps (see Table 1). The hip starts from a flexed position and then extends throughout stance, which, in combination with the extension–flexion moment around the hip (Fig. 6), results in the support leg in power generation followed by absorption.

## DISCUSSION

### Mechanics at the whole-body level: BCOM and GRFs

Spontaneous overground WRT was characterized by a sudden increase in forward speed during the transition step, the so-called speed jump. The approach towards spontaneous gait transition was characterized by an acceleration of  $0.5 \text{ ms}^{-2}$ , but during the transition step (0.49 s; see supplementary material Table S1) there was a sudden increase in speed of  $0.42 \text{ ms}^{-2}$ , implying an instantaneous acceleration of  $0.85 \text{ ms}^{-2}$ , almost doubling the acceleration of the previous walking steps. This is in agreement with the larger net propulsive force impulse during step 0, due to a smaller braking impulse during the first part of stance in step 0. The initial contact phase in walking and running [even in accelerated walking (Orendurff et al., 2008) and running (Van Caekenberghe et al., 2013)] is indeed characterized by a decrease in the forward velocity of the BCOM because the BCOM is

Table 1. Statistical comparison of work delivered during identified power phases in stance

ANOVA		ANOVA step	Step -2	Step -1	Step 0	Step +1	
Ankle	A1	0.000	0.203±0.067* <sup>§</sup>	0.305±0.126* <sup>§</sup>	0.530±0.086 <sup>†</sup>	0.670±0.158 <sup>†</sup>	
	Knee	K1	0.004	0.047±0.026* <sup>§</sup>	0.044±0.029* <sup>§</sup>	0.014±0.006 <sup>†</sup> <sup>§</sup>	0.113±0.064 <sup>†</sup> <sup>*</sup>
		K2	0.001	-0.021±0.021* <sup>§</sup>	-0.038±0.028* <sup>§</sup>	-0.288±0.076 <sup>†</sup>	-0.205±0.146 <sup>†</sup>
Hip	K3	0.001	0.124±0.069 <sup>†</sup> <sup>*§</sup>	0.187±0.064 <sup>†</sup> <sup>*§</sup>	0.606±0.226 <sup>†</sup>	0.687±0.239 <sup>†</sup>	
	H1	0.011	0.359±0.235*	0.233±0.146 <sup>§</sup>	0.150±0.113 <sup>§</sup>	0.370±0.149 <sup>†</sup> <sup>*</sup>	
	H2	0.238	-0.432±0.221	-0.467±0.160	-0.350±0.272	-0.553±0.195	

Work data ( $\text{J kg}^{-1}$ ) are means ± s.d.

A1, positive work by the ankle extensors during push-off; K1, positive work by the knee flexors at initial contact; K2, negative work by the knee extensors; K3, positive work by the knee extensors; H1, positive work by the hip extensors; H2, power absorption by the hip flexors.

<sup>†</sup>Significant difference from step -2; <sup>†</sup>significant difference from step -1; \*significant difference from step 0; <sup>§</sup>significant difference from step +1.

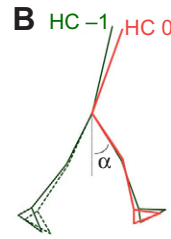
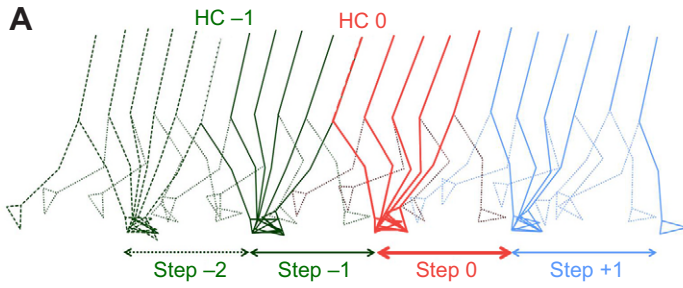


Fig. 4. Kinematics of the spontaneous overground WRT (based upon the mean kinematics,  $N=17$ ). (A) Dashed/solid lines indicate the stance limb, dotted lines the swinging leg. (B) A comparison of the configuration at heel contact of step -1 (HC -1) and step 0 (HC 0).  $\alpha$  indicates the forward thigh rotation in the sagittal plane.

positioned behind the centre of pressure. The smaller braking impulse, followed by an equal propulsive impulse in the transition step (compared with the previous walking steps), resulted in a net horizontal speed increase accounting for 83% of the gain in energy at the BCOM level (the so-called energy jump of  $0.83 \text{ J kg}^{-1}$  during the entire step 0). During the transition step there was an increase not only in horizontal speed but also in BCOM vertical energy (vertical position and speed of BCOM) from touchdown to take

off. This is the net effect of a decrease in potential and vertical kinetic energy during the first phase of stance in step 0, followed by an increase in vertical height of the BCOM and an increase in vertical kinetic energy at toe-off that is necessary to generate the first flight phase of running. Concurrently, the vertical GRF pattern during stance changed from a double hump pattern in the walking steps before step 0 towards a running-like single hump pattern in step 0. As such, both the in-phase BCOM energy fluctuations and

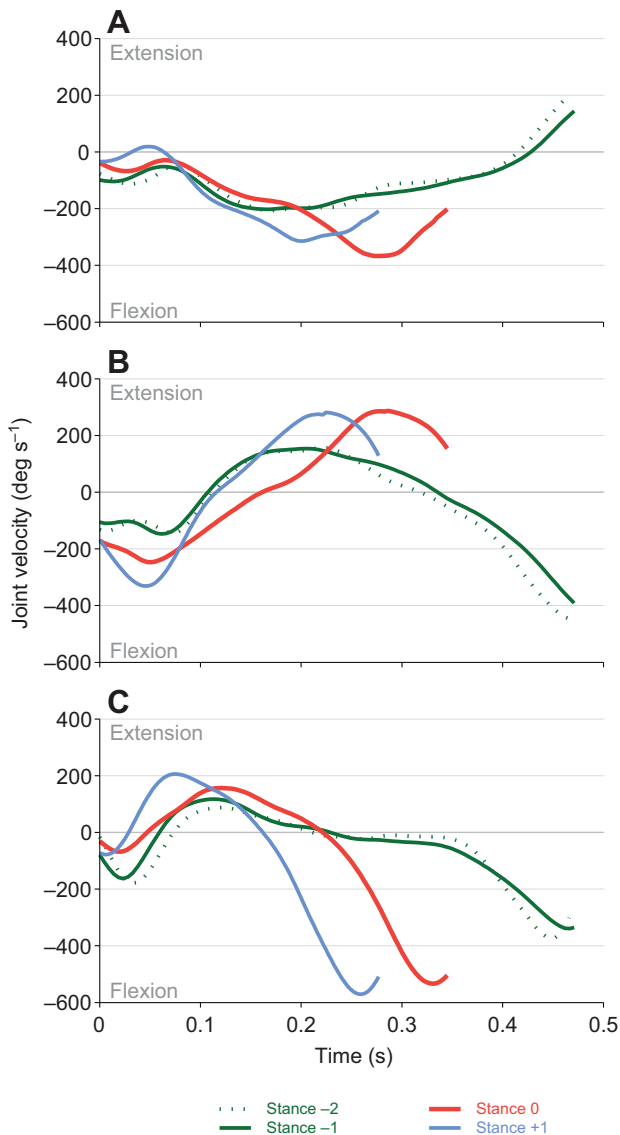


Fig. 5. Joint velocity during stance. (A) Hip, (B) knee and (C) ankle.

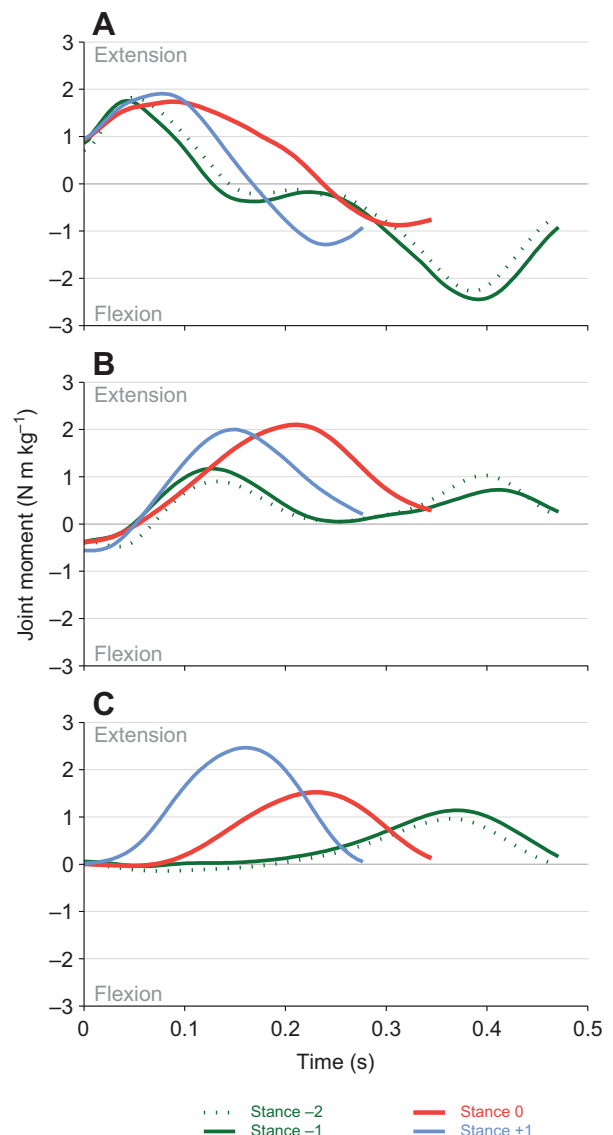


Fig. 6. Joint moment during stance. (A) Hip, (B) knee and (C) ankle.

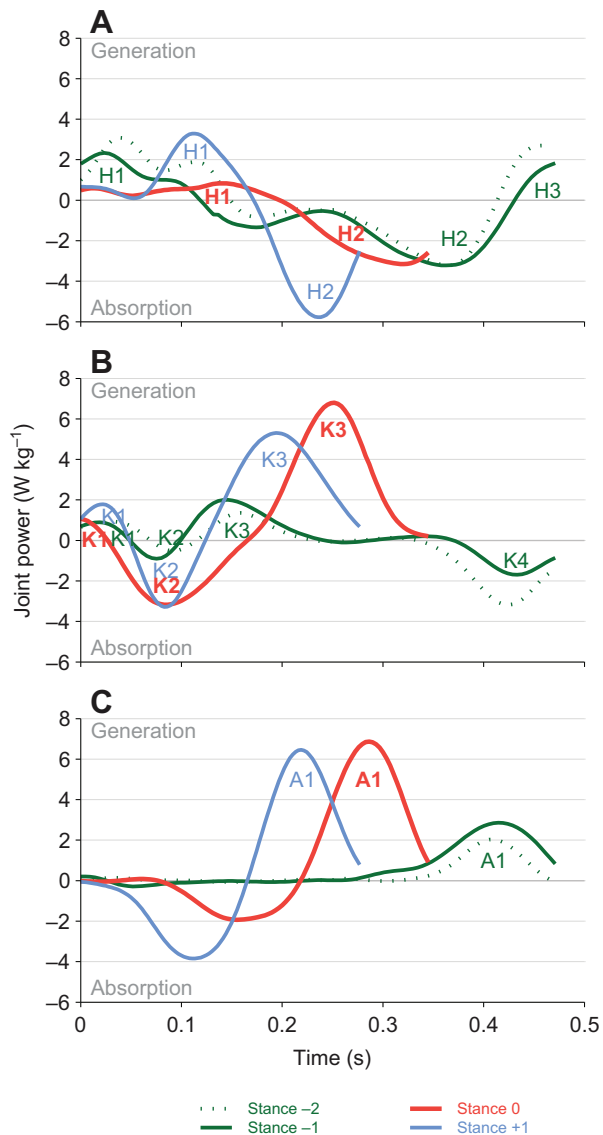


Fig. 7. Joint power during stance. (A) Hip, (B) knee and (C) ankle. Joint power profiles during stance were divided into phases following Winter (Winter, 1983; Winter, 1987). Only power phases that were present in both walking and running were taken into account (see Fig. 6). These accord with joint activation as follows: A1, concentric propulsive plantar flexion of the ankle at the end of stance; K1, eccentric knee extensor activity early in stance (loading response); K2, concentric knee extensor activity during mid-stance; K3, eccentric activity in the rectus femoris at the end of stance; K4, a region of negative power, corresponding to eccentric activity in the hamstrings during terminal swing; H1, concentric hip extensor activity early in stance (loading response, sometimes absent); H2, eccentric hip flexor activity during mid-stance; H3, a region of positive power, corresponding to concentric activity in the hip flexors during preswing and initial swing.

the vertical GRF pattern already feature a ‘bouncing’ running-like stance phase of step 0.

Nevertheless, focusing on the ‘propulsion’ phase of step 0 (defined as ‘after zero crossing of the horizontal GRF’), the increase of  $1.22 \text{ J kg}^{-1}$  of all three BCOM energy components is larger than the  $0.83 \text{ J kg}^{-1}$  net energy increase during entire stance. This suggests a motor reorganization, which combines reduced braking followed by a more ‘energetic’ take off.

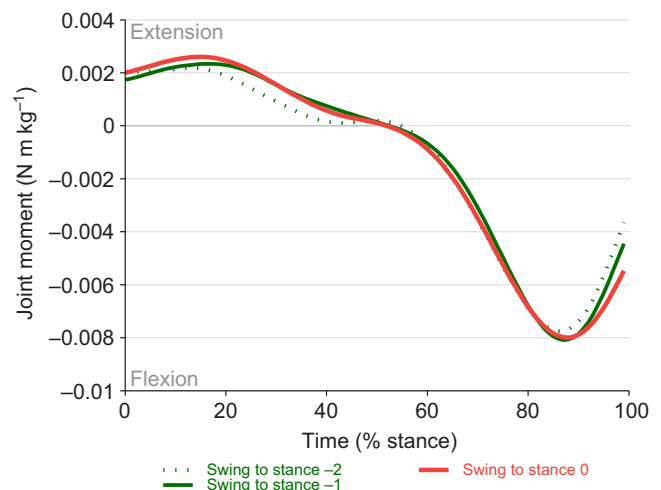


Fig. 8. Knee moment during swing.

### How do we realize this net speed–energy jump?

#### The decrease in braking impulse

As shown in Fig. 2 and by the statistics presented in the Results, the speed jump during the transition step was caused by a significant decrease in the braking impulse and not by an increase in the propulsive impulse. A prerequisite for a smaller braking impulse is that the body is positioned in an optimal kinematic configuration to avoid braking forces. Indeed, the landing configuration at heel contact of step 0 (Fig. 4B) was characterized by an increased flexion of the knee and hip joints of the transition step stance leg compared with the preceding walking steps stance leg. These altered landing conditions were prepared by kinematic adaptations during the last 40% of swing prior to the transition step (supplementary material Fig. S5). Because of these changes, the BCOM is still situated behind the centre of pressure, but is already 4 cm closer to it at heel contact in comparison to step -1, hence probably explaining the smaller braking forces.

Additionally, there is still a small double support phase at the start of step 0 meaning that the ankle push off at the contralateral foot (the trailing foot, at the end of the stance phase of step -1) helps to attenuate the braking at the initial contact of step 0 (Kuo, 2007). In this context, the somewhat larger (trend to significance,  $P=0.078$ ) concentric ankle work (Fig. 7C, A1 phase; Table 1) in step -1 compared with step -2 also contributes to less braking upon touchdown of step 0.

#### Altered landing configuration

How does the ‘more flexed’ configuration of the hip and knee compare with the landing configuration of the previous step? The increased hip flexion was due to a more forward rotation of the trunk and thigh (Fig. 4B). The more forward inclined trunk was associated with the increased hip flexion moment during the second phase of stance of the previous walking step (i.e. the contralateral legs’ side in step -1, Fig. 6A). As the hip flexion moment at the swing leg side was equal to that during the previous walking step, the more pronounced forward thigh rotation was not due to a larger hip flexion moment but was caused by the larger knee flexion. Indeed, the latter produced a smaller overall inertia of the swing leg during the last 40% of swing. This was caused by a larger knee flexion moment (Fig. 8), which decelerated the extension movement

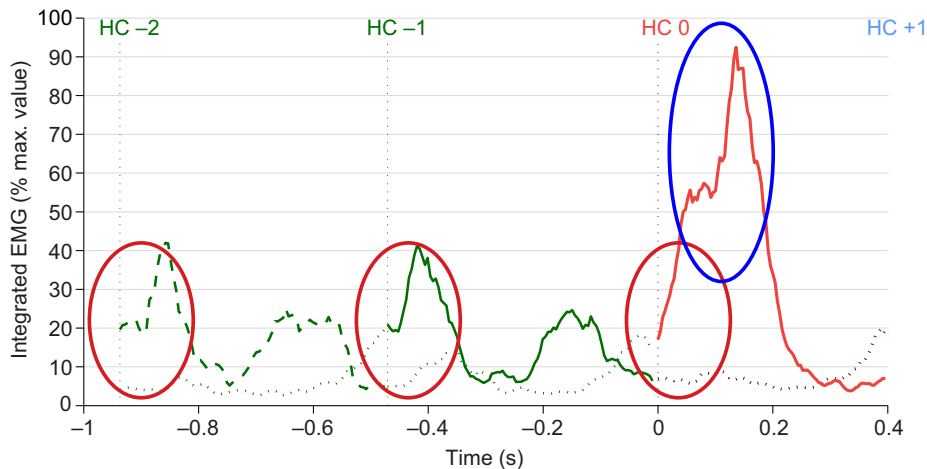


Fig. 9. Electromyogram of step -2, -1 and 0 for the stance limb (dashed and full line) and swing limb (dotted line). Time 0 is the heel contact (HC) transition step.

of the knee during final swing to a larger extent, and thus led to reduced knee extension (i.e. larger flexion). This decelerated extension of the swing leg is probably realized by eccentric work of the hamstring muscles, and might assist in obtaining a smaller braking impulse. The same mechanism can also be observed in the clawing touchdown during sprinting (Hunter et al., 2005), which assists in minimizing the braking impulse required to accelerate.

#### Propulsion

After zero crossing of the horizontal GRF, an energy jump of  $1.2 \text{ J kg}^{-1}$  was observed. During the propulsive phase of the transition step, this work has to be delivered to generate the vertical and horizontal impulse needed for the transition (Fig. 2).

The push-off of the transition step is related to a powerful ankle and knee extension, power absorption at the hip and power generation by the contralateral swing leg. The work related to the ankle extension contributes as much as the work related to the knee extension (see Table 1, A1 and K3). However, compared with the preceding accelerating walking steps, a more drastic increase in work is observed in the knee compared to the ankle. Ankle plantar flexion work increases with a factor of 1.65; knee extension rises with a factor of 3 during the transition step.

The tripling of the power generated by the knee is not a coincidental finding. We hypothesize that this is a consequence of the altered landing configuration of the knee. As a result of flexion of the knee, the GRF moment arm around the knee becomes larger at initial contact of the transition step, compared with heel strikes of the preceding walking steps. Assuming that the swinging limb is still naive (i.e. in 'walking mode'), the decreased knee stiffness associated with this larger knee flexion at heel contact (Farley et al., 1998; Lafortune et al., 1996) in combination with the larger moment arm can cause further flexion of the knee during stance. *Post hoc* tests with five subjects, measuring EMG during spontaneous WRT, indeed showed that knee extensors are naive to the altered landing condition (pre-activation identical to preceding walking steps; see red ellipses in Fig. 9). This is also reflected in the identical joint moments (pointing towards a similar input from the higher control level towards the muscle). As a consequence, the largely identical initial loading of the limb (see loading rates immediately after heel strike in Fig. 2) must result in a sudden deeper knee flexion, rapidly stretching the mono-articular knee extensors. We hypothesize that this evokes the typical stretch reflex, which increases motor activation of the knee extensors. As a result, (1) knee flexion will

first be slowed down and (2) a more powerful extension during the second half of stance will occur so that the body is launched in the first flight phase of the running gait. Upon landing, the body proceeds in its bouncing gait.

Indirect evidence in support of this hypothesis is provided in two ways: Fig. 9 shows that *m. vastus* activation levels, while initially not different from the preceding walking steps, increased rapidly beyond walking level (Fig. 9, blue ellipsis), and vertical GRFs show a small plateau coinciding with the peak in knee flexion velocity (compare Fig. 2B with Fig. 5B) suggesting a temporarily reduced resistance to gravity (i.e. the resilient limb) followed, however, by a force increase when the limbs stiffens as a result of the increased extensor activity.

If correct, this causal chain may also explain the abrupt switch from the inverted pendular to the spring-mass energy exchange mechanism (see also Segers et al., 2007b): increased extensor activity during knee flexion may be indicative of elastic loading of the spring elements of the muscle-tendon system. Recoil during the second part of stance (when GRFs decrease again) can thus assist in powering of the first flight phase.

#### Finalization of the WRT

In order to evoke a spontaneous WRT transition, the current study adopted the same protocol as used previously (De Smet et al., 2009b). The transition speed of  $2.73 \text{ m s}^{-1}$  and comparable spatio-temporal profile reinforce the findings of previous research and indicate that indeed a repeatable execution of the WRT was studied.

The question remains of whether the reorganization of the locomotor system is completed after the transition step. Although we did not compare the first and second running step after the WRT with a running step during a constant run, we feel we gathered enough indirect evidence to make this assumption. The consistency of the spatiotemporal parameters after transition (constant speed, step length and step frequency) (Segers et al., 2006) in combination with the lack of kinematic differences between step +1 and step +2 indicates a completion of the transition after the transition stride.

#### CONCLUSION

The mechanical and kinesiological variables, measured continuously during spontaneous WRTs, show a sudden spatio-temporal switch, within one transition step, from walking to running. At total body level, a sudden increase in energy of the BCOM and an abrupt change from an out-of-phase to an in-phase organization of the

energy fluctuations occurs. These observations concur with the changes in the GRF pattern during stance phase, with the largest net propulsive impulse during the transition step and a vertical GRF pattern that suddenly changes from a walking pattern, over a one-step intermediate, to a running pattern. It is probable that the altered landing configuration (prepared during the last 40% of the preceding swing only) that places the body in an optimal configuration to minimize braking impulse also evokes a reflex that enables a more powerful push off, generating enough power to complete the transition and to launch the first flight phase.

#### ACKNOWLEDGEMENTS

The authors acknowledge Ir J. Gerlo and Ir D. Spiessens for data collection and technical support, and Dr P. Malcolm and Dr F. Deconinck for professional advice.

#### AUTHOR CONTRIBUTIONS

V.S. and K.D.S. contributed equally to this work.

#### COMPETING INTERESTS

No competing interests declared.

#### FUNDING

This research was funded by Fund for Scientific Research Flanders [grant no. FWO B/08892/01 to K.D.S.; F6/15DPG.0183.09 to P.A. and D.D.C.; 08/ASP/152 to I.V.C.] and the European Community's Seventh Framework Programme FP7/2007-2013 – Future Emerging Technologies, Embodied Intelligence, under grant agreement no. 231688.

#### REFERENCES

- De Smet, K., Malcolm, P., Lenoir, M., Segers, V. and De Clercq, D. (2009a). Effects of optic flow on spontaneous overground walk-to-run transition. *Exp. Brain Res.* **193**, 501-508.
- De Smet, K., Segers, V., Lenoir, M. and De Clercq, D. (2009b). Spatiotemporal characteristics of spontaneous walk-to-run transition. *Gait Posture* **29**, 54-58.
- Diedrich, F. J. and Warren, W. H., Jr (1995). Why change gaits? Dynamics of the walk-run transition. *J. Exp. Psychol. Hum. Percept. Perform.* **21**, 183-202.
- Farley, C. T. and Ferris, D. P. (1998). Biomechanics of walking and running: center of mass movements to muscle action. *Exerc. Sport Sci. Rev.* **26**, 253-285.
- Farley, C. T., Houdijk, H. H. P., Van Strien, C. and Louie, M. (1998). Mechanism of leg stiffness adjustment for hopping on surfaces of different stiffnesses. *J. Appl. Physiol.* **85**, 1044-1055.
- Ganley, K. J., Stock, A., Herman, R. M., Santello, M. and Willis, W. T. (2011). Fuel oxidation at the walk-to-run-transition in humans. *Metabolism* **60**, 609-616.
- Hreljac, A. (1993). Preferred and energetically optimal gait transition speeds in human locomotion. *Med. Sci. Sports Exerc.* **25**, 1158-1162.
- Hreljac, A., Imamura, R. T., Escamilla, R. F. and Edwards, W. B. (2007). When does a gait transition occur during human locomotion? *J. Sport Sci. Med.* **6**, 36-43.
- Hreljac, A., Imamura, R. T., Escamilla, R. F., Edwards, W. B. and MacLeod, T. (2008). The relationship between joint kinetic factors and the walk-run gait transition speed during human locomotion. *J. Appl. Biomech.* **24**, 149-157.
- Hunter, J. P., Marshall, R. N. and McNair, P. J. (2005). Relationships between ground reaction force impulse and kinematics of sprint-running acceleration. *J. Appl. Biomech.* **21**, 31-43.
- Ivanenko, Y. P., Poppele, R. E. and Lacquaniti, F. (2006). Spinal cord maps of spatiotemporal alpha-motoneuron activation in humans walking at different speeds. *J. Neurophysiol.* **95**, 602-618.
- Kuo, A. D. (2007). The six determinants of gait and the inverted pendulum analogy: a dynamic walking perspective. *Hum. Mov. Sci.* **26**, 617-656.
- Lafortune, M. A., Hennig, E. M. and Lake, M. J. (1996). Dominant role of interface over knee angle for cushioning impact loading and regulating initial leg stiffness. *J. Biomech.* **29**, 1523-1529.
- Lee, S. J. and Hidler, J. (2008). Biomechanics of overground vs. treadmill walking in healthy individuals. *J. Appl. Physiol.* **104**, 747-755.
- Li, L. (2000). Stability landscapes of walking and running near gait transition speed. *J. Appl. Biomech.* **16**, 428-435.
- Li, L. and Hamill, J. (2002). Characteristics of the vertical ground reaction force component prior to gait transition. *Res. Q. Exerc. Sport* **73**, 229-237.
- Nimbarde, A. D. and Li, L. (2011). Effect of added weights on the characteristics of vertical ground reaction force during walk-to-run gait transition. *Hum. Mov. Sci.* **30**, 81-87.
- Nishikawa, K., Biewener, A. A., Aerts, P., Ahn, A. N., Chiel, H. J., Daley, M. A., Daniel, T. L., Full, R. J., Hale, M. E., Hedrick, T. L. et al. (2007). Neuromechanics: an integrative approach for understanding motor control. *Integr. Comp. Biol.* **47**, 16-54.
- Orendurff, M. S., Bernatz, G. C., Schoen, J. A. and Klute, G. K. (2008). Kinetic mechanisms to alter walking speed. *Gait Posture* **27**, 603-610.
- Priulsky, B. I. and Gregor, R. J. (2001). Swing- and support-related muscle actions differentially trigger human walk-run and run-walk transitions. *J. Exp. Biol.* **204**, 2277-2287.
- Raynor, A. J., Yi, C. J., Abernethy, B. and Jong, Q. J. (2002). Are transitions in human gait determined by mechanical, kinetic or energetic factors? *Hum. Mov. Sci.* **21**, 785-805.
- Segers, V., Aerts, P., Lenoir, M. and De Clercq, D. (2006). Spatiotemporal characteristics of the walk-to-run and run-to-walk transition when gradually changing speed. *Gait Posture* **24**, 247-254.
- Segers, V., Lenoir, M., Aerts, P. and De Clercq, D. (2007a). Kinematics of the transition between walking and running when gradually changing speed. *Gait Posture* **26**, 349-361.
- Segers, V., Aerts, P., Lenoir, M. and De Clercq, D. (2007b). Dynamics of the body centre of mass during actual acceleration across transition speed. *J. Exp. Biol.* **210**, 578-585.
- Thorstensson, A. and Rotherthson, H. (1987). Adaptations to changing speed in human locomotion: speed of transition between walking and running. *Acta Physiol. Scand.* **131**, 211-214.
- Turvey, M. T., Holt, K. G., LaFandra, M. E. and Fonseca, S. T. (1999). Can the transition to and from running and the metabolic cost of running be determined from the kinetic energy of running? *J. Mot. Behav.* **31**, 265-278.
- Van Caekenberghe, I., Segers, V., De Smet, K., Aerts, P. and De Clercq, D. (2010a). Influence of treadmill acceleration on actual walk-to-run transition. *Gait Posture* **31**, 52-56.
- Van Caekenberghe, I., De Smet, K., Segers, V. and De Clercq, D. (2010b). Overground vs. treadmill walk-to-run transition. *Gait Posture* **31**, 420-428.
- Van Caekenberghe, I., Segers, V., Willems, P., Gosseye, T., Aerts, P. and De Clercq, D. (2013). Mechanics of overground accelerated running vs. running on an accelerated treadmill. *Gait Posture* **38**, 125-131.
- Winter, D. A. (1983). Moments of force and mechanical power in jogging. *J. Biomech.* **16**, 91-97.
- Winter, D. A. (1991). *The Biomechanics and Motor Control of Human Gait: Normal, Elderly and Pathological*. Waterloo, ON: Waterloo Biomechanics.



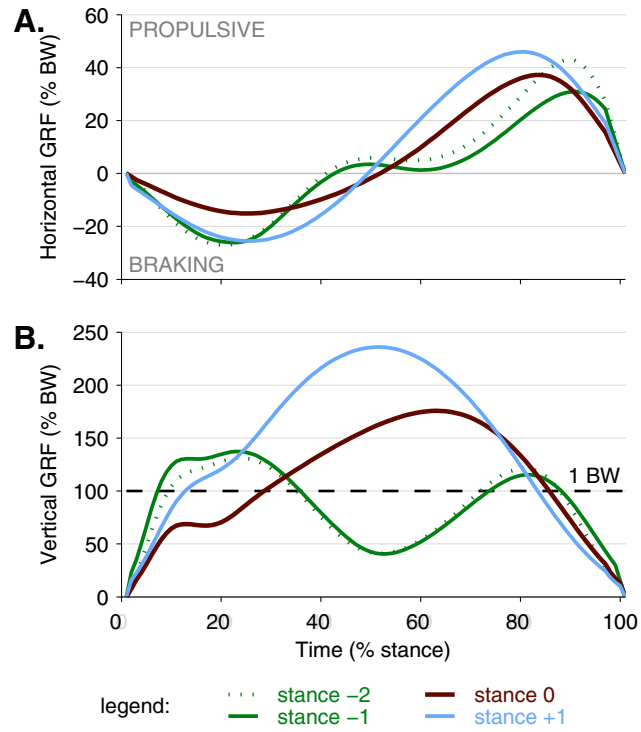


**Fig. S1.** Ground reaction forces during the spontaneous WRT. A. Horizontal (fore-aft) ground reaction forces. B. Vertical ground reaction forces.

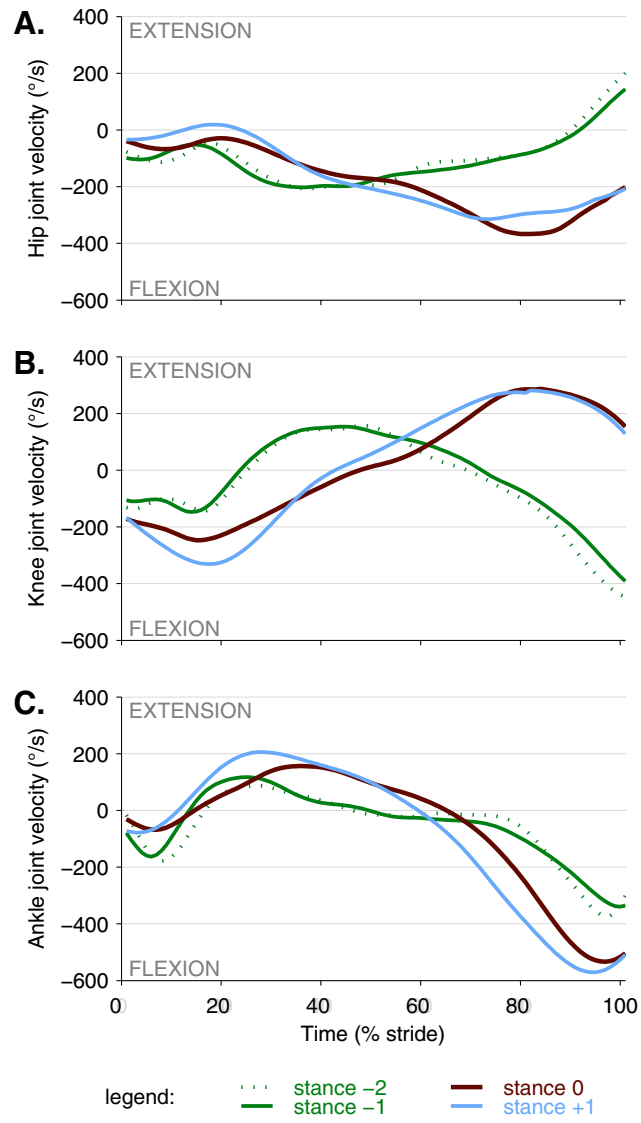


**Fig. S2.** Joint velocity during stance. A. Hip, B. knee, C. ankle .

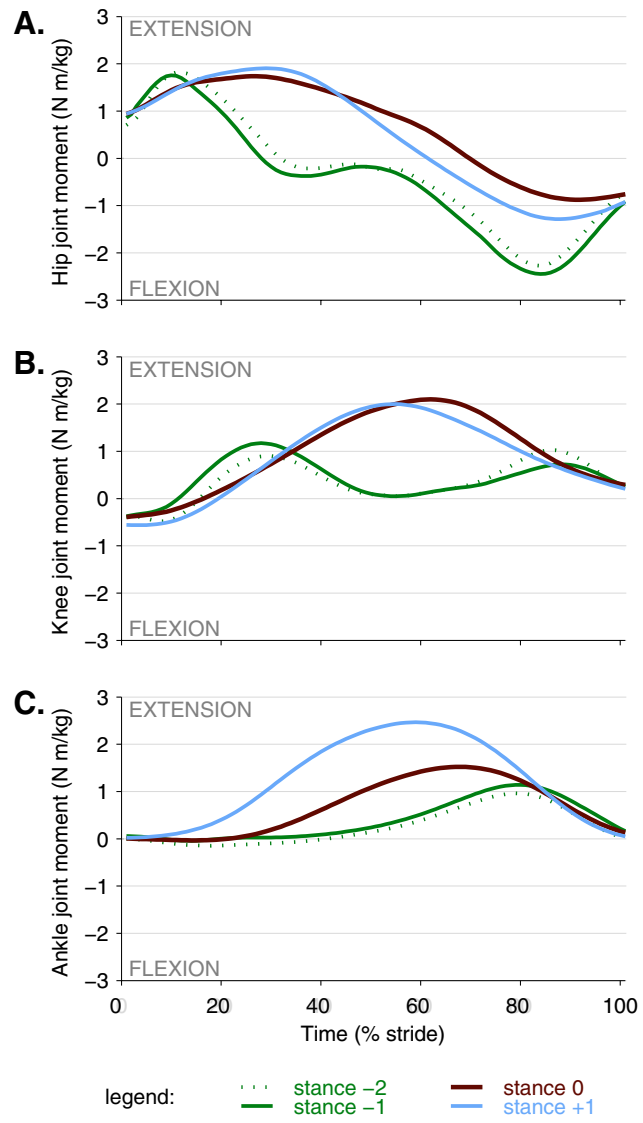
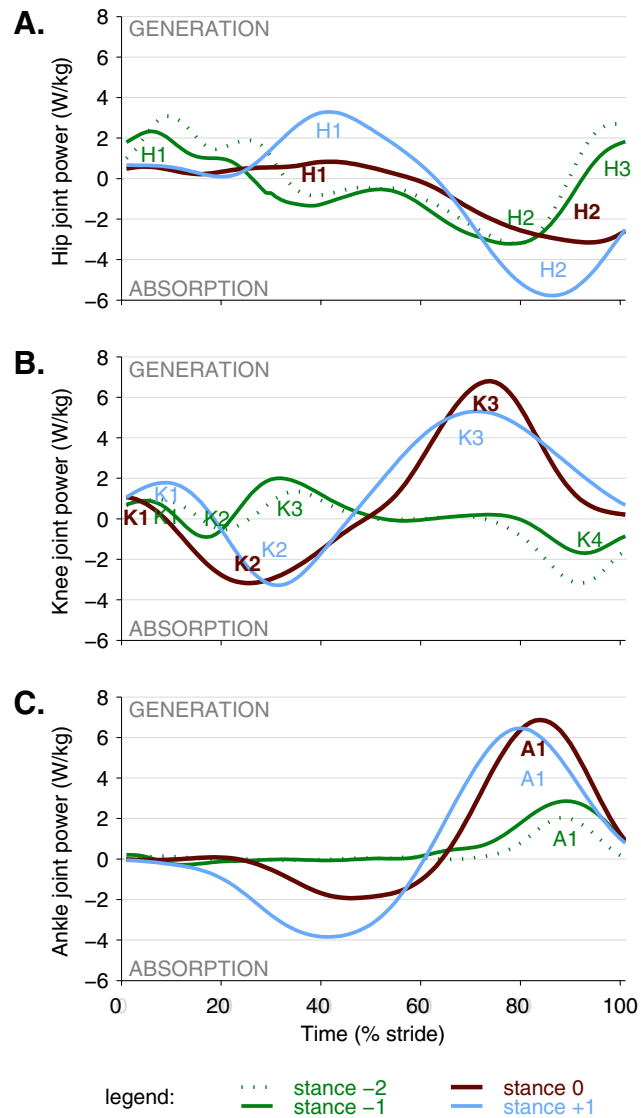
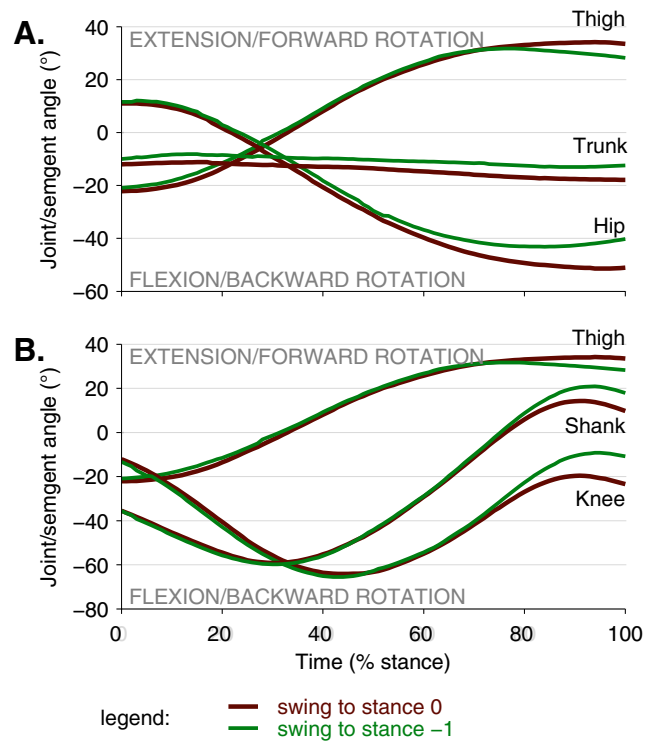


Fig. S3. Joint moment during stance. A. Hip, B. knee, C. ankle.



**Fig. S4.** Joint power during stance. A. Hip, B. Knee, C. Ankle. Joint power profiles during stance are divided in phases following Winter (1983, 1987). Only power phases that were present in both walking and running were taken into account (see figure 6). These accord to joint activation as follows: A1, concentric propulsive plantar flexion of the ankle at the end of stance; K1, eccentric knee extensor activity early in stance (loading response); K2, concentric knee extensor activity during midstance; K3, eccentric activity in the rectus femoris at the end of stance; H1, concentric hip extensor activity early in stance (loading response, sometimes absent); H2, eccentric hip flexor activity during midstance.



**Fig. S5.** Kinematics of the swing phase towards step -1 (green) and step 0 (red). A. Segment angles of thigh and trunk, and the resulting hip joint angle. B. Segment angles of shank and thigh, and the resulting knee joint angle.

	step -2		step -1		step 0		step +1	
	mean	s.d.	mean	s.d.	mean	s.d.	mean	s.d.
Step length (m)	0.91	± 0.06	0.96	± 0.07	1.20	± 0.13	1.16	± 0.14
Step frequency (Hz)	2.34	± 0.18	2.42	± 0.19	2.30	± 0.16	2.59	± 0.14
Speed (m/s)	2.13	± 0.21	2.32	± 0.20	2.74	± 0.25	2.98	± 0.34

**Table S1. Spatiotemporal realization of the spontaneous overground walk-to-run transition.**